Published in final edited form as:
Invest Ophthalmol Vis Sci. 2002 September ; 43(9): 3045–3052.

Hemodynamic Parameters in Blood Vessels in Choroidal Melanoma Xenografts and Rat Choroid

Rod D. Braun[1,2], **Asad Abbas**[1], **S. Omar Bukhari**[3], and **Willie Wilson III**[3]

1 *Department of Anatomy and Cell Biology, Wayne State University School of Medicine, Detroit, Michigan*

2 *Barbara Ann Karmanos Cancer Institute, Wayne State University, Detroit, Michigan*

3 *Department of Radiation Oncology, Duke University Medical Center, Durham, North Carolina*

Abstract

Purpose— Choroidal melanoma is the most common primary ocular cancer among the adult population. To avoid enucleation, there has been a concerted effort to develop therapies that spare the affected eye and the patient's vision. Blood flow helps shape the tumor's microenvironment, plays a key role in the tumor's response to many different types of therapy, and is necessary for delivery of chemotherapeutic agents. To rationally design new therapies and optimize existing treatments, it is essential to learn as much as possible about blood flow and the microcirculation in this tumor. In recent years, much has been discovered about the anatomy of the microvasculature and the dynamics of overall blood flow in choroidal melanoma, but little is known about the factors that determine microvascular blood flow. In this study hemodynamic parameters in individual microvessels of a human choroidal melanoma xenograft were compared with those same parameters in a normal rat choroid.

Methods— Nude, athymic WAG/*RijHs-rnu* rats were used in this study. The human choroidal melanoma cell line OCM-1 was used to grow solid tumors subcutaneously in the flanks of donor rats. Small pieces of these tumors were then implanted into the choroidal space of recipient rats. After 6 to 8 weeks, the rats were anesthetized with a subcutaneous injection of urethane, and the sclera was exposed. Rhodamine-labeled li-posomes and red blood cells (RBCs) labeled with 1,1′-dioctadecyl-3,3,3′,3′-tetramethylindocarbocyanine perchlorate (DiI) were injected intravenously. Epifluorescent, intravital microscopy was used to visualize the flow of fluorescent RBCs through individual vessels in the choroid or tumor. Flow through multiple vessels was recorded on videotape for later analysis. From the recordings, *RBC flux*, RBC velocity (V_c), and microvascular hematocrit (HCT_m) were determined. Similar experiments were performed in rats with no tumor growth, and these same parameters were calculated in normal choroidal vessels. RBC flow was characterized in 55 vessels in six OCM-1 tumors and in 153 choroidal vessels in five non–tumor-bearing rats.

Results—*RBC flux* was higher in larger tumor vessels (>30 m in diameter) compared with similarly sized choroidal vessels. There were no differences in the velocities of RBCs through the two types of vessels. HCT_m was significantly higher in medium-sized (>20 m in diameter) and larger tumor vessels compared with normal choroidal vessels.

Conclusions— These experiments demonstrate differences between hemodynamic parameters in normal choroidal microvessels and microvessels in choroidal melanoma in this animal model. Because HCT_m is a key determinant of apparent viscosity, abnormally high HCT_m in the tumor

[1] Corresponding author: Rod D. Braun, Anatomy and Cell Biology, Wayne State University School of Medicine, 540 E. Canfield Avenue, Detroit, MI 48201; rbraun@med.wayne.edu.

Commercial relationships policy: N.

Supported by National Eye Institute Grant EY11634.

vessels would increase vascular resistance and decrease flow. This could have a negative impact on the tumor oxygen levels and on the ability to deliver drugs effectively. On the contrary, higher local HCT_m has also been shown to increase oxygen delivery. The impact and interplay of these two effects on tumor oxygenation remain to be determined.

Choroidal melanoma is a solid tumor arising from choroidal melanocytes. Although the occurrence of this tumor is relatively rare compared with other types of cancer, it is the most common adult primary intraocular malignancy, accounting for 70% of all primary intraocular eye cancers.[1] Its dangerous metastatic potential makes it of special concern to ophthalmologists. The median survival after a diagnosis of metastasis is only 4 to 7 months.[2,3]

Despite significant research effort, there is still a need for improved treatment of choroidal melanoma. The two most commonly used treatments for medium-sized tumors are enucleation or radiation therapy. Although radiation therapy spares the eye, vision may be adversely affected. In one report, only 36% of all patients maintained visual acuity better than 6/12 three years after radiation therapy.[4] Because of this risk of treatment-related vision loss, there has been a recent trend to optimize radiation therapy[5] and to investigate more local, conservative, eye-sparing therapies.[6] The ultimate goals of any treatment of choroidal melanoma should be eradication of the primary tumor, prevention of metastatic spread, and maintenance of the patient's vision.

To improve existing therapies and to develop new, vision-sparing treatments for choroidal melanoma, it is necessary to gather detailed information about the blood supply and microcirculation in this tumor. Not only is blood flow essential for tumor growth and metastasis, it is also a major factor in a tumor's response to many therapies. Delivery of chemotherapeutic drugs is dependent on the distribution of blood flow within the tumor and the permeability of the vasculature.[7] The efficacy of some therapies is affected by the microenvironment within the tumor, which is shaped by the blood flow, among other factors. For example, several different forms of cancer therapy are dependent on tumor oxygen levels, including radiation therapy[8] and photodynamic therapy.[9] In addition, some chemotherapeutic drugs (hypoxic cytotoxins) are sensitive to the oxygen level and are much more effective under hypoxic conditions.[10] Therefore, information about the blood flow characteristics of a specific tumor is imperative before rationally designing new therapies or optimizing existing treatments.

Over the past decade, there has been an increased effort to study blood flow and vascular architecture in choroidal melanoma. Beginning in the early 1990s, attempts were made to measure global blood flow in choroidal melanomas in patients by means of color Doppler imaging.[11,12] More recently, the technique was used to measure blood velocity and vascular resistance in the major ocular arteries in patients with choroidal melanoma before and after radiotherapy.[13] The most interesting findings have been in the area of vascular architecture. In 1993, Folberg et al.[14] identified nine different vascular patterns in histologic sections of choroidal melanoma and determined that the presence of loops and networks was correlated with poor prognosis. Subsequent work suggested that these network patterns were composed of extracellular matrix–lined channels generated by the tumor cells themselves in a process called vasculogenic mimicry.[15] This link between vascular pattern and prognosis has stimulated an interest in imaging the microvasculature of choroidal melanoma in patients. In 1995, indocyanine green videoangiography was used to evaluate vascular patterns in choroidal tumors.[16] More recently, confocal indocyanine green angiography has been used to visualize the microcirculation and to identify vascular patterns in experimental and clinical choroidal melanoma.[17,18]

Although this information about the architecture of the blood vessels and overall blood flow in the tumor is extremely important, there is still little or no knowledge about the factors that help determine the microvascular flow properties in choroidal melanoma. In general, tumors are characterized by chaotic vascular networks and very heterogeneous, unstable blood flow.[19,20] One of the causes of this abnormal blood flow is high viscous resistance within the tumor vasculature.[20] The viscous resistance is a function of hemodynamic parameters in the microvessels (e.g., the microvascular hematocrit [HCT_m]).[21] In a review in 1988, Jain[20] stressed the need to measure the microvascular hematocrit and other rheologic parameters within individual tumor microvessels to better understand the factors that determine the tumor's overall blood flow. In the current study, we determined the hemodynamic parameters in blood vessels in a human choroidal melanoma xenograft model and compared them with those found in normal choroidal blood vessels. We hypothesized that there are differences in the blood flow properties between choroidal melanoma microvessels and normal choroidal microvessels. Specifically, we hypothesized that HCT_m would be higher in the microvessels of choroidal melanoma than in vessels in the normal choroid.

METHODS

Animals

The mutant rat strain WAG/*RijHs-rnu* was used in this study for two reasons. First, these rats are athymic, which permits the xenotransplantation of human tumor tissue into the rat. Second, they are albino, which allows normal choroidal vessels and tumor vessels to be viewed with epifluorescence. The rats were bred and housed at the Duke University Cancer Center Isolation Facility. All procedures were in accordance with the ARVO Statement for the Use of Animals in Ophthalmic and Vision Research and were approved by the Duke University Institutional Animal Care and Use Committee.

Because there is no information in the literature on the blood parameters in the WAG/*RijHs-rnu* rat strain, blood from four rats was subjected to standard, manual hematologic measurements. Total erythrocyte concentration was $6.98 \pm 0.95 \times 10^6$ cells/L (mean ± SD, $n = 4$), total leukocyte count was 12,951 ± 3,720 cells/L, and the mean corpuscular volume (*MCV*) was 60.1 ± 0.1 m^3.

Maintenance of the Choroidal Melanoma Cell Line OCM-1

The OCM-1 human choroidal melanoma cell line used in this project was the kind gift of June Kan-Mitchell (Wayne State University School of Medicine, Detroit, MI). The cells were grown and maintained in RPMI medium with 10% fetal calf serum.[22] The originally supplied cells were grown in tissue culture and split. The resultant generations of cells were frozen and stored. These stock cells were used to generate the tumor cells used in subsequent transplantations. All the cells used were within three generations of this stock. Tumor pieces for transplantation into the choroid were obtained from subcutaneous tumors, grown in donor rats. While the rat was lightly restrained, 0.2 mL OCM-1 cell suspension (50×10^6 cells/mL) was injected subcutaneously into the back. After 2 to 4 weeks, an approximately 1-cm-diameter tumor was evident at the injection site.

Tumor Implantation into Choroid

The method of tumor implantation was similar to that used by Mueller et al.,[17] who implanted pieces of subcutaneously grown OCM-1 tumor into the choroids of rabbits. The donor rat, bearing the subcutaneous tumor, was heavily anesthetized with an intraperitoneal injection of pentobarbital sodium (70 mg/kg). The tumor was excised and placed in sterile RPMI medium. Viable tumor pieces, as indicated by their firmness and pink color, were minced with a scalpel and a 30-gauge needle. After removal of the tumor, the donor rat was killed with an overdose

of pentobarbital sodium. Recipient rats were anesthetized with intramuscular injection of a ketamine-xylazine mixture (50/5.3 mg/kg) and sterile proparacaine HCl (0.5%) was applied topically to the right eye as local anesthesia. The rat was placed under an operating scope, and the sclera was exposed. A small tunnel was made in the sclera with a 30-gauge needle. A spatula constructed from a 30-gauge needle was used to insert an approximately 0.5-mm^3 piece of OCM-1 tumor from the donor rat into the tunnel. The scleral pocket was sealed with surgical glue (Nexaband; Veterinary Product Laboratories, Phoenix, AZ), and ophthalmic antibiotic ointment (Vetropolycin; Pharmaderm, Melville, NY) was applied. After recovery, the rat was returned to its cage and checked daily for signs of infection.

Fluorescent Markers

Several different fluorescent markers were used in this work. Rhodamine-labeled, sterically stabilized, long-circulating, pegylated liposomes were injected to visualize plasma in the blood vessels. These liposomes consisted of egg phosphatidylcholine, cholesterol, 1,2-dis-tearoyl-*sn*-glycero-3-phosphoethanolamine-*N*-polyethylene glycol 2000, and lissamine rhodamine B 1,2-dihexadecanoyl-*sn*-glycero-3-phospho-ethanolamine (rhodamine-DHPE) in a molar ratio of 10:5:0.8:0.1.[23] All lipids except the rhodamine-DHPE were purchased from Avanti Polar Lipids (Alabaster, AL). Rhodamine-DHPE was purchased from Molecular Probes (Eugene, OR). The liposomes were prepared by the lipid film hydration and extrusion method.[24] The resultant liposomes had a diameter of approximately 200 nm, with a final lipid concentration after hydration of 20 mg/mL.

Red blood cells (RBCs) for labeling were obtained from donor rats in the colony. The RBCs were labeled with 1,1′-dioctadecyl-3,3,3,3′-tetramethylindocarbocyanine perchlorate (DiI; Molecular Probes) by a technique that has been described in detail elsewhere.[25] Briefly, after blood was removed from the donor rat, RBCs were isolated by successive washing and centrifugation. Then 100 L of RBCs was incubated for 30 minutes in a mixture of 10 mL PBS and 100 L 0.5 mg/mL DiI in ethanol. After washing and centrifugation, 100 L DiI-labeled RBCs (DiI-RBCs) was resuspended in 1 mL PBS for a final concentration of 100 L DiI-RBCs/mL.

Videomicroscopy of Choroidal or Tumor Circulation

The exposure of the sclera to permit microscopic observation of the choroidal or tumor circulation has been described elsewhere.[26] All rats were anesthetized with subcutaneously injected urethane (1.5 g/kg; 240 mg/mL urethane in water), and surgery was begun only after surgical anesthesia had been achieved (1–2 hours). The femoral artery and vein were cannulated so that arterial blood pressure could be monitored, and the fluorescent markers could be infused, respectively.

Observation of individual choroidal blood vessels has also been described in detail.[26] Briefly, the rat was positioned in a head holder and placed on the stage of an intravital microscope (Axiskop; Carl Zeiss, Thornwood, NY). The eye was positioned under the 20× long-working-distance objective. A drop of hydroxypropyl methylcellulose 2.5% (Goniosol; Novartis Ophthalmics, Duluth, GA) was applied to the sclera, and a piece of glass coverslip approximately 5 × 5 mm was positioned to serve as a contact lens.

Small volumes (0.2 mL) of rhodamine-labeled liposomes and DiI-RBCs (0.1–0.2 mL) were injected intravenously. Fluorescence microscopy was performed with epi-illumination by a 100-W mercury source with the appropriate filter set. The set had a band-pass excitation filter ($\lambda = 540 – 550$ nm) and a long-pass emission filter ($\lambda \geq 590$ nm). Images were recorded with a silicon-intensified tube (SIT) video camera (model C2400-08; Hamamatsu, Hamamatsu City, Japan) connected to an S-VHS video recorder (model BV-1000; NEC-Mitsubishi Electronics,

Itasca, IL). A video timer signal (model VTG-55; For-A, Los Angeles, CA) was superimposed on the images for record keeping. During epi-illumination, a suitable region of the choroid or tumor was located, and the field was videotaped for later analysis. After the experiments, a blood sample was taken from the arterial catheter for determination of the labeled fraction of RBCs by flow cytometry (FACScan; BD Biosciences, Franklin Lakes, NJ). The labeled fraction is the relative number of RBCs that carry the DiI label (number of DiI RBCs/total number of RBCs).

Analysis of Videotape Images and Determination of Microvascular Parameters

The videotapes were analyzed, and microvascular parameters were determined as described previously.[26] Vascular fields in which at least 60 seconds of RBC transit was recorded were identified. In each field, vessels were traced onto a sheet of transparency film taped onto a high-resolution video monitor, and the number of DiI-RBCs entering each vessel during 60 seconds was counted to give the flux of DiI-RBCs per minute. The *RBC flux* was then determined by dividing the DiI-*RBC flux* by the labeled fraction.

The same video image was then viewed in slow motion, and velocities of the DiI-RBC were determined by calculating the transit time of the cells across the length of the vessel. Velocities were determined for a maximum of 25 DiI-RBCs for the 1-minute period, and the mean cell velocity (V_c) was calculated. Vascular diameters were determined in individual image frames of each vascular field captured and digitized from the videotape (Simple PCI C-Imaging System; Compix, Inc., Lake Oswego, OR). The digital image was imported into a computer (ScionImage software; Scion, Gaithersburg, MD), and the diameter of each vessel was measured at four positions along its length. The average of the measurements was used as the vascular diameter (d) in subsequent calculations. HCT_m was calculated using the following established equation[27]

$$HCT_m = \frac{(MCV)(RBC\ \ flux)}{\pi \frac{d^2}{4}(V_c)}$$

MCV was set at 60 m^6, as determined from the blood analysis.

Statistics

Correlations between each hemodynamic parameter and vessel diameter were determined by standard linear regression analysis. Comparisons of the hemodynamic parameters in each diameter range were made with the nonparametric Mann-Whitney test. Differences were considered statistically significant if $P < 0.05$.

RESULTS

Visualization of OCM-1 Tumor Growing in Rat Choroid

Tumor growth was evident in the choroid after 6 to 8 weeks, although there were usually no gross external signs of tumor growth (e.g., protrusion of the eye). The tumor could be easily visualized under low magnification with epifluorescence microscopy after infusion of the rhodamine-labeled liposomes (Fig. 1A). The general outline of the tumor could be distinguished, and the tumor mass was usually elevated above the choroidal vessels. In the example shown in Figure 1A, normal choroidal vessels can be seen entering or exiting the tumor mass in the top left of the photograph (Fig. 1A, arrows). The white box denotes the region viewed under high magnification in Figure 1B. This field was used to analyze erythrocyte flow, and two RBCs can be seen flowing through the central vessel (Fig. 1B, arrows).

RBC Flux in Normal Choroid and Choroidal Melanoma

One hundred fifty-three normal choroidal vessels were analyzed in five rats, which had a mean (± SD) blood pressure of 89 ± 9 mm Hg during the measurements. *RBC flux* varied from less than 100 to nearly 3500 RBCs/sec (Fig. 2A). There was a statistically significant positive correlation between the *RBC flux* and vessel diameter ($r^2 = 0.556$, $P < 0.0001$). Figure 2B shows similar data for the 55 vessels analyzed in choroidal melanoma in six rats. The mean blood pressure in these rats was 86 ± 6 mm Hg. As was the case for the normal choroidal vessels, there was a significant positive correlation between the flux and the diameter ($r^2 = 0.464$, $P < 0.0001$). The flux ranged from several hundred RBCs/sec in 10- to 20-m-diameter vessels to well over 4000 RBCs/sec in some of the largest vessels. When the mean and median values were calculated for each range of vessel diameter and the two vascular networks were compared, there was no significant difference in *RBC flux* between smaller vessels in normal choroid and those in choroidal melanoma, although there was a trend for more RBCs to flow through tumor vessels of similar size (Table 1, Fig. 3). In vessels with diameters between 30 and 45 m, the *RBC flux* was significantly higher in the OCM-1 tumor than in the normal choroid ($P = 0.0002$).

RBC Velocity in Normal Choroid and Choroidal Melanoma

In normal choroidal vessels, most RBCs flowed at a velocity between 0.2 and 1.5 mm/sec (Fig. 4A). There was a weak, but statistically significant, positive correlation between RBC velocity and diameter ($r^2 = 0.089$ $P = 0.0002$). The range of RBC velocity in most vessels in choroidal melanoma was similar to that in choroidal vessels (Fig. 4B), although there was no correlation between RBC velocity and diameter in the tumor vessels ($r^2 = 0.003$; $P = 0.679$). When the RBC velocities in the different diameter ranges were compared, there were no significant differences between the velocities in tumor vessels and those in normal choroidal vessels (Table 1, Fig. 3).

HCT_m in Normal Choroid and Choroidal Melanoma

HCT_m ranged from approximately 5% to 65% in most vessels in the normal choroid and was negatively correlated with vessel diameter (Fig. 5A; $r^2 = 0.295$, $P < 0.0001$). In most blood vessels in choroidal melanoma, HCT_m ranged from 12% to 70% (Fig. 5B). There was a weak negative correlation between HCT_m and vessel diameter ($r^2 = 0.104$, $P = 0.016$). When HCT_m was compared between the two tissues at different diameter ranges, the hematocrit in tumor vessels with diameters greater than 20 m was significantly higher than in normal choroidal vessels of similar size (Table 1, Fig. 3).

DISCUSSION

Model of Human Choroidal Melanoma for Intravital Microscopy

The experimental model presented in this work was designed to permit microscopic observation of individual blood cells in the microvessels of human choroidal melanoma xenografts. To accomplish this goal, several compromises were necessary. First, because the visualization relies on epifluorescence microscopy, it was necessary to minimize absorption of light by the tissue. This was accomplished by using albino rats and the amelanotic human choroidal melanoma cell line OCM-1. Therefore, this model does not exactly mimic the clinical condition, because most choroidal melanomas are pigmented. Another necessary compromise was the use of nude, athymic rats. These rats did not reject the human tumor tissue and permitted growth of the xenografts without the need for immunosuppressants. Unfortunately, the use of nude rats made routine monitoring of tumor growth more difficult, because the animals could not be removed from the isolation facility for observation.

Another limitation of this current model is the method of tumor implantation. Although the choroidal melanoma grew orthotopically in the choroid, it arose from a fragment taken from a subcutaneously grown OCM-1 tumor. Therefore, the implanted OCM-1 cells could have been altered by growing first in the subcutaneous site. With other tumor types, it has been demonstrated that the site of growth can affect vessel density and permeability[28] and gene expression.[29] In addition, the subcutaneous tissue fragments implanted into the choroid may have contained dermal rat microendothelial cells that could have contributed to angiogenesis of the tumor in the choroid. Thus, the model may not exactly simulate the microcirculation of clinical human uveal melanoma. In future studies, we will attempt to use a model in which the choroidal melanomas are derived directly from the tumor cell suspension.

Despite these weaknesses, the model permitted the visualization of single blood cells in individual blood vessels, and hemodynamic parameters were quantified in microvessels of choroidal melanoma for the first time. In the future, this model could be used to study the impact of radiotherapy or antiangiogenic therapy on the microvascular bed. In addition, the impact of various agents (e.g., oxygen or drugs) on microvascular blood flow could be determined.

Hemodynamic Parameters in Choroid

The hemodynamic parameters measured in the normal choroid were in general agreement with those found in a prior study in the choroid of Sprague-Dawley rats.[26] Although the correlations between the various parameters and diameter were the same in the two studies, there were some differences in the absolute values. In this study, RBC velocity was lower than in the Sprague-Dawley choroidal vessels, and hematocrit was higher. Because the same anesthetic regimen was used and none of the other methods were changed, this discrepancy is most likely attributable to some inherent difference between the Sprague-Dawley rats and the WAG/*RijHs -rnu* nude rats.

RBC flux in OCM-1 Choroidal Melanoma

In blood vessels of the OCM-1 tumor, *RBC flux* tended to be higher than in normal choroidal vessels across the entire diameter range, but the difference was only statistically significant in vessels with diameters of more than 30 m (Fig. 3A, Table 1). In a study comparing hemodynamic parameters in R3230Ac mammary adenocarcinoma and in normal granulation tissue, it was also found that *RBC flux* in tumor vessels was significantly higher than in similarly sized normal vessels.[30] The most likely explanation for higher *RBC flux* in tumor vessels compared with normal vessels is a difference in branching patterns in the two vascular beds. Tumor vessels are highly tortuous and disorganized[31] and often exhibit sparse branching patterns.[32] In contrast, the choroidal circulation is distinguished by a highly organized lobular architecture.[33] On the arterial side, tumor vessels may branch less than normal choroidal vessels, which would lead to higher *RBC flux* in the daughter vessels of the tumor-supplying arterioles. On the venous side, the tumor venules may collect blood from more small venules or capillaries than from the choroidal venules. This would lead to a higher *RBC flux* in the tumor-collecting venules.

Not only is the pattern of vascularization heterogeneous in tumors, but the composition and origin of the vessels within the tumor can be very different.[34] This is particularly true of the blood vessels in choroidal melanoma. Some choroidal melanomas may contain a mixture of vessel types, including vessels incorporated from the choroid and channels lined by extracellular matrix.[35] These channels arise from the tumor cells themselves through a process termed vasculogenic mimicry.[15] Whether *RBC flux* and the other hemodynamic parameters would be different in endothelium-lined vessels than in vasculogenic vessels is not clear. This

question was not investigated in the present study, and no attempt was made to determine the composition of the vessels that were analyzed.

RBC Velocity in OCM-1 Choroidal Melanoma

Unlike the weak correlation found between RBC velocity and vessel diameter in the normal choroid, there was no significant correlation between velocity and diameter in choroidal melanoma vessels (Fig. 4B). This noncorrelation has been reported previously for blood vessels in other tumors.[28,36]

Tumor vessel RBC velocity was not significantly different from the velocity in choroidal vessels of similar size (Fig. 3B, Table 1). This finding is consistent with other studies that show no difference between erythrocyte velocities in tumor and normal vessels.[30,37] Alternatively, there have been other reports that RBC or blood velocities in tumor vessels are lower than in normal tissue vessels.[36,38] Most likely, the relative RBC velocity in tumor vessels is dependent on the type of tumor and its site of growth.

HCT_m in OCM-1 Choroidal Melanoma

In the OCM-1 choroidal melanoma, HCT_m was always higher than 10% and was significantly higher than that in normal choroid (Fig. 3C, Table 1). To the best of our knowledge, this is only the second measurement of HCT_m in tumor vessels. HCT_m was also measured in the microvessels of rat mammary adenocarcinoma grown in the rat dorsal window chamber model. [30] Tumor vessel HCT_m was not different from HCT_m in normal granulation tissue vessels. In that study the range of tumor vessel diameters observed was only between 13 and 23 m. In the present study, HCT_m in that same diameter range was also not different in tumor and normal choroidal vessels (Fig. 3C, Table 1). HCT_m in the OCM-1 tumor was significantly higher than HCT_m in the normal choroid only when vessels greater than 20 m in diameter were considered. The abnormally high HCT_m is most likely attributable to the severe hemoconcentration that occurs in tumors. It has been reported that as blood passes through the tumor vasculature, it loses 5% to 14% of the plasma, and the hematocrit of the venous blood is increased by approximately 5%.[39–41] This means that there is high plasma leakage in the tumor vasculature without the reabsorption of plasma that occurs in most tissues.

Hemoconcentration and poor plasma reabsorption most likely account for the weak, negative correlation between tumor HCT_m and vessel diameter (Fig. 5B) as well. This negative correlation is atypical of most circulations. The choroid is the only vasculature in which such a correlation has been found.[26] In cat mesentery,[42] rat mesentery,[43] and rat cremaster muscle, [44] a positive correlation exists. In hamster cheek pouch vessels, no correlation between HCT_m and vessel diameter was found, and there was large variability in HCT_m.[27] It has been suggested that the negative correlation in the choroid was most likely caused by fluid movement across the choroidal vessel walls.[26] It has been postulated that there is a shift in the transition point from filtration to absorption far to the venous side of the choroidal circulation. Thus, smaller vessels lost plasma and became hemoconcentrated, but the plasma was reabsorbed by the larger venous vessels, and HCT_m decreased as the diameter increased. In the tumor, there is severe loss of plasma and hemoconcentration, but little reabsorption.[39–41] Therefore, the *HCT* in all vessels is very high, and the correlation with vessel diameter is very weak.

Implications of High HCT_m

The very high HCT_m in tumor vessels has several important implications. First, there could be a large, negative impact on the tumor's blood flow. It is already known that overall flow resistance is increased in tumors and that the increase is at least partly attributable to the tortuosity and other architectural abnormalities of the tumor's vessels.[20] Another factor that affects vascular resistance is blood rheology, and there is some evidence that the apparent

viscosity of blood within microvessels in the tumor is increased.[45] Because HCT_m is a key determinant of apparent viscosity,[21] the high HCT_m in the tumor may help explain this reported increase in blood viscosity. This negative impact on blood flow would not be the only effect of elevated HCT_m on a choroidal melanoma's physiology. In addition to increasing viscosity, higher local HCT_m has also been shown to increase oxygen delivery, because oxygen delivery depends on spacing of the RBCs.[46] Therefore, the overall impact of the high HCT_m on the microenvironment of choroidal melanoma is a balance between a decrease in blood flow and an enhancement of oxygen delivery.

These physiologic consequences of high HCT_m could have significance in several treatment options for choroidal melanoma. If the high flow resistance indeed results in decreased blood flow in the tumor and in lower oxygen levels within the tumor, the efficacy of radiotherapy and photodynamic therapy would be greatly reduced, because both depend on local oxygen levels.[8,9] Studies are currently under way in the laboratory to determine oxygen levels in the OCM-1 choroidal melanoma and to investigate methods of modifying blood flow in this tumor model.

References

1. Sahel JA, Albert DM. Intraocular melanomas. Cancer Treat Res 1993;65:161–199. [PubMed: 8104021]
2. Gragoudas ES, Egan KM, Seddon JM, et al. Survival of patients with metastases from uveal melanoma. Ophthalmology 1991;98:383–389. [PubMed: 2023760]
3. Einhorn LH, Burgess MA, Gottlieb JA. Metastatic patterns of choroidal melanoma. Cancer 1974;34:1001–1004. [PubMed: 4424282]
4. Char DH, Kroll S, Quivey JM, Castro J. Long term visual outcome of radiated uveal melanomas in eyes eligible for randomisation to enucleation versus brachytherapy. Br J Ophthalmol 1996;80:117–124. [PubMed: 8814740]
5. Finger PT. Radiation therapy for choroidal melanoma. Surv Ophthalmol 1997;42:215–232. [PubMed: 9406368]
6. De Potter P, Shields CL, Shields JA. New treatment modalities for uveal melanoma. Curr Opin Ophthalmol 1996;7:27–32. [PubMed: 10163456]
7. Jain RK. Delivery of molecular and cellular medicine to solid tumors. J Control Release 1998;53:49–67. [PubMed: 9741913]
8. Gray LJ, Conger AD, Ebert M, Hornsey S, Scott OCA. The concentration of oxygen dissolved in tissues at the time of irradiation as a factor in radiotherapy. Br J Radiol 1953;26:638–648. [PubMed: 13106296]
9. Chapman JD, Stobbe CC, Arnfield MR, Santus R, Lee J, McPhee MS. Oxygen dependency of tumor cell killing in vitro by light-activated Photofrin II. Radiat Res 1991;126:73–79. [PubMed: 1826959]
10. Brown JM, Giaccia AJ. Tumour hypoxia: the picture has changed in the 1990s. Int J Radiat Biol 1994;65:95–102. [PubMed: 7905916]
11. Wolff-Kormann PG, Kormann BA, Riedel KG, et al. Quantitative color Doppler imaging in untreated and irradiated choroidal melanoma. Invest Ophthalmol Vis Sci 1992;33:1928–1933. [PubMed: 1374744]
12. Lieb WE, Shields JA, Cohen SM, et al. Color Doppler imaging in the management of intraocular tumors. Ophthalmology 1990;97:1660–1664. [PubMed: 2087296]
13. Vecsei PV, Kircher K, Nagel G, et al. Ocular arterial blood flow of choroidal melanoma eyes before and after stereotactic radiotherapy using Leksell gamma knife: 2 year follow up. Br J Ophthalmol 1999;83:1324–1328. [PubMed: 10574807]
14. Folberg R, Rummelt V, Parys-Van Ginderdeuren R, et al. The prognostic value of tumor blood vessel morphology in primary uveal melanoma. Ophthalmology 1993;100:1389–1398. [PubMed: 8371929]
15. Maniotis AJ, Folberg R, Hess A, et al. Vascular channel formation by human melanoma cells in vivo and in vitro: vasculogenic mimicry. Am J Pathol 1999;155:739–752. [PubMed: 10487832]

16. Shields CL, Shields JA, De Potter P. Patterns of indocyanine green videoangiography of choroidal tumours. Br J Ophthalmol 1995;79:237–245. [PubMed: 7703202]
17. Mueller AJ, Folberg R, Freeman WR, et al. Evaluation of the human choroidal melanoma rabbit model for studying microcirculation patterns with confocal ICG and histology. Exp Eye Res 1999;68:671–678. [PubMed: 10375430]
18. Mueller AJ, Freeman WR, Folberg R, et al. Evaluation of microvascularization pattern visibility in human choroidal melanomas: comparison of confocal fluorescein with indocyanine green angiography. Graefes Arch Clin Exp Ophthalmol 1999;237:448 –456. [PubMed: 10379603]
19. Chaplin DJ, Hill SA, Bell KM, Tozer GM. Modification of tumor blood flow: current status and future directions. Semin Radiat Oncol 1998;8:151–163. [PubMed: 9634492]
20. Jain RK. Determinants of tumor blood flow: a review. Cancer Res 1988;48:2641–2658. [PubMed: 3282647]
21. Pries AR, Neuhaus D, Gaehtgens P. Blood viscosity in tube flow: dependence on diameter and hematocrit. Am J Physiol 1992;263:H1770 –H1778. [PubMed: 1481902]
22. Kan-Mitchell J, Mitchell MS, Rao N, Liggett PE. Characterization of uveal melanoma cell lines that grow as xenografts in rabbit eyes. Invest Ophthalmol Vis Sci 1989;30:829 –834. [PubMed: 2722439]
23. Yuan F, Dellian M, Fukumura D, et al. Vascular permeability in a human tumor xenograft: molecular size dependence and cutoff size. Cancer Res 1995;55:3752–3756. [PubMed: 7641188]
24. Hope MJ, Bally MB, Webb G, Cullis PR. Production of large unilamellar vesicles by a rapid extrusion procedure: characterization of size, trapped volume and ability to maintain a membrane potential. Biochim Biophys Acta 1985;812:55–65.
25. Unthank JL, Lash JM, Nixon JC, Sidner RA, Bohlen HG. Evaluation of carbocyanine-labeled erythrocytes for microvascular measurements. Microvasc Res 1993;45:193–210. [PubMed: 8361402]
26. Braun RD, Dewhirst MW, Hatchell DL. Quantification of erythrocyte flow in the choroid of the albino rat. Am J Physiol 1997;272:H1444 –H1453. [PubMed: 9087623]
27. Sarelius IH, Duling BR. Direct measurement of microvessel hematocrit, red cell flux, velocity, and transit time. Am J Physiol 1982;243:H1018 –H1026. [PubMed: 7149038]
28. Fukumura D, Yuan F, Monsky WL, Chen Y, Jain RK. Effect of host microenvironment on the microcirculation of human colon adenocarcinoma. Am J Pathol 1997;151:679 –688. [PubMed: 9284816]
29. Greene GF, Kitadai Y, Pettaway CA, von Eschenbach AC, Bucana CD, Fidler IJ. Correlation of metastasis-related gene expression with metastatic potential in human prostate carcinoma cells implanted in nude mice using an in situ messenger RNA hybridization technique. Am J Pathol 1997;150:1571–1582. [PubMed: 9137084]
30. Brizel DM, Klitzman B, Cook JM, Edwards J, Rosner G, Dewhirst MW. A comparison of tumor and normal tissue microvascular hematocrits and red cell fluxes in a rat window chamber model. Int J Radiat Oncol Biol Phys 1993;25:269 –276. [PubMed: 8420874]
31. Less JR, Skalak TC, Sevick EM, Jain RK. Microvascular architecture in a mammary carcinoma: branching patterns and vessel dimensions. Cancer Res 1991;51:265–273. [PubMed: 1988088]
32. Falk P. The vascular pattern of the spontaneous C3H mouse mammary carcinoma and its significance in radiation response and in hyperthermia. Eur J Cancer 1980;16:203–217. [PubMed: 7371678]
33. Yoneya S, Tso MO, Shimizu K. Patterns of the choriocapillaris: a method to study the choroidal vasculature of the enucleated human eye. Int Ophthalmol 1983;6:95–99. [PubMed: 6403481]
34. Chang YS, di Tomaso E, McDonald DM, Jones R, Jain RK, Munn LL. Mosaic blood vessels in tumors: frequency of cancer cells in contact with flowing blood. Proc Natl Acad Sci USA 2000;97:14608 –14613. [PubMed: 11121063]
35. Folberg R, Hendrix MJ, Maniotis AJ. Vasculogenic mimicry and tumor angiogenesis. Am J Pathol 2000;156:361–381. [PubMed: 10666364]
36. Funakoshi N, Onizuka M, Yanagi K, et al. A new model of lung metastasis for intravital studies. Microvasc Res 2000;59:361–367. [PubMed: 10792967]
37. Schmidt J, Ryschich E, Maksan SM, et al. Influence of gastrointestinal hormones on tumor microcirculation of experimental pancreatic cancer in the rat. Dig Surg 2000;17:250 –255. [PubMed: 10867458]

38. Peyman GA, Khoobehi B, Moshfeghi A, et al. Blood velocity in an experimental iris tumor. Ophthalmic Surg Lasers 1998;29:506–509. [PubMed: 9640574]
39. Butler TP, Grantham FH, Gullino PM. Bulk transfer of fluid in the interstitial compartment of mammary tumors. Cancer Res 1975;35:3084 –3088. [PubMed: 1182701]
40. Sevick EM, Jain RK. Blood flow and venous pH of tissue-isolated Walker 256 carcinoma during hyperglycemia. Cancer Res 1988;48:1201–1207. [PubMed: 3342400]
41. Vaupel P, Kallinowski F. Hemoconcentration of blood flowing through human tumor xenografts (Abstract). Int J Microcirc Clin Exp 1987;6:72.
42. Lipowsky HH, Usami S, Chien S. In vivo measurements of “apparent viscosity” and microvessel hematocrit in the mesentery of the cat. Microvasc Res 1980;19:297–319. [PubMed: 7382851]
43. Kanzow G, Pries AR, Gaehtgens P. Analysis of the hematocrit distribution in the mesenteric microcirculation. Int J Microcirc Clin Exp 1982;1:67–79. [PubMed: 7188443]
44. House SD, Lipowsky HH. Microvascular hematocrit and red cell flux in rat cremaster muscle. Am J Physiol 1987;252:H211–H222. [PubMed: 3812711]
45. Sevick EM, Jain RK. Viscous resistance to blood flow in solid tumors: effect of hematocrit on intratumor blood viscosity. Cancer Res 1989;49:3513–3519. [PubMed: 2731173]
46. Federspiel WJ, Sarelius IH. An examination of the contribution of red cell spacing to the uniformity of oxygen flux at the capillary wall. Microvasc Res 1984;27:273–285. [PubMed: 6727699]

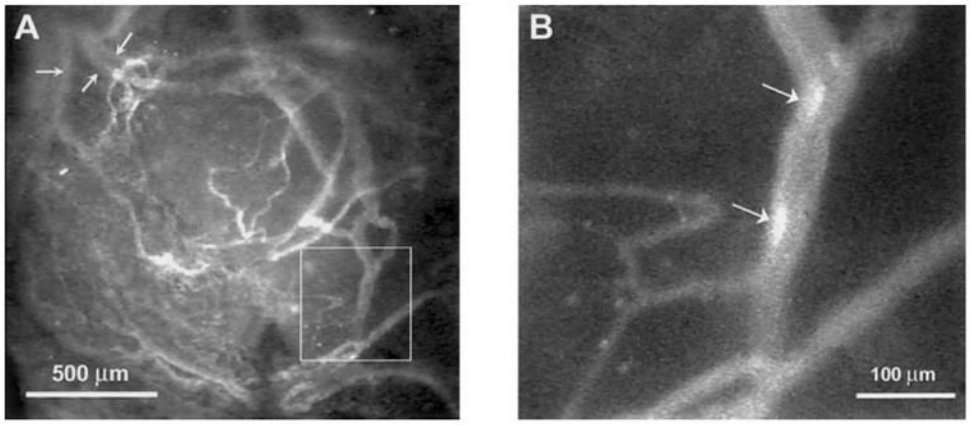

Figure 1.
Low-magnification epi-fluorescent image of an OCM-1 tumor growing in the choroid of an athymic rat (**A**). The vessels contain fluorescently labeled liposomes. *Arrows*: normal choroidal vessels entering or exiting the tumor mass. *Box*: region of the tumor shown at higher magnification in (**B**). (**B**, *arrows*) Two DiI-labeled RBCs flowing through the vessel.

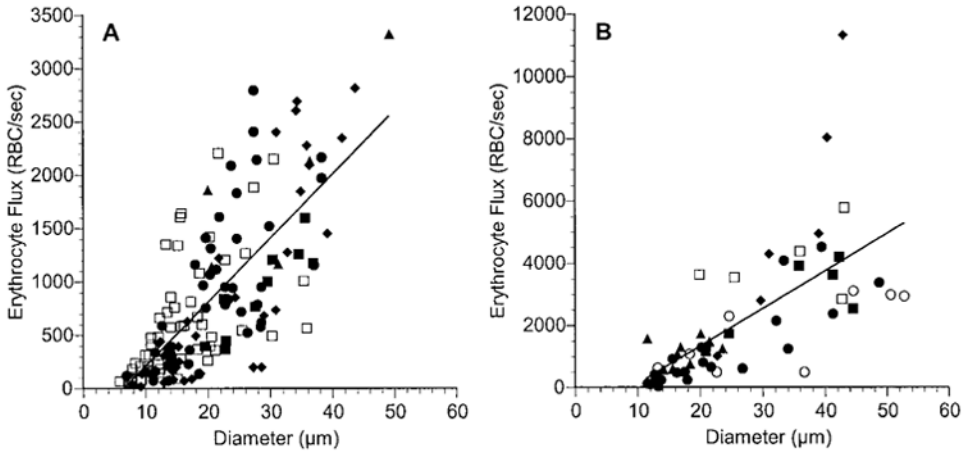

Figure 2.

RBC flux as a function of vessel diameter in normal choroid (**A**) and in choroidal melanoma (**B**). Each rat is denoted by a different *symbol*, and each *symbol* represents a separate vessel. *Solid line*: the linear regression for the data from all the rats. In normal choroid: *RBC flux* = 60.0 × diameter − 396.4, $n = 153$ vessels in five rats, $r = 0.746$, $P < 0.0001$. In choroidal melanoma: *RBC flux* = 120.7 × diameter − 1102.1, $n = 55$ vessels in six rats, $r = 0.681$, $P < 0.0001$. Note that the scales on the ordinate axes differ.

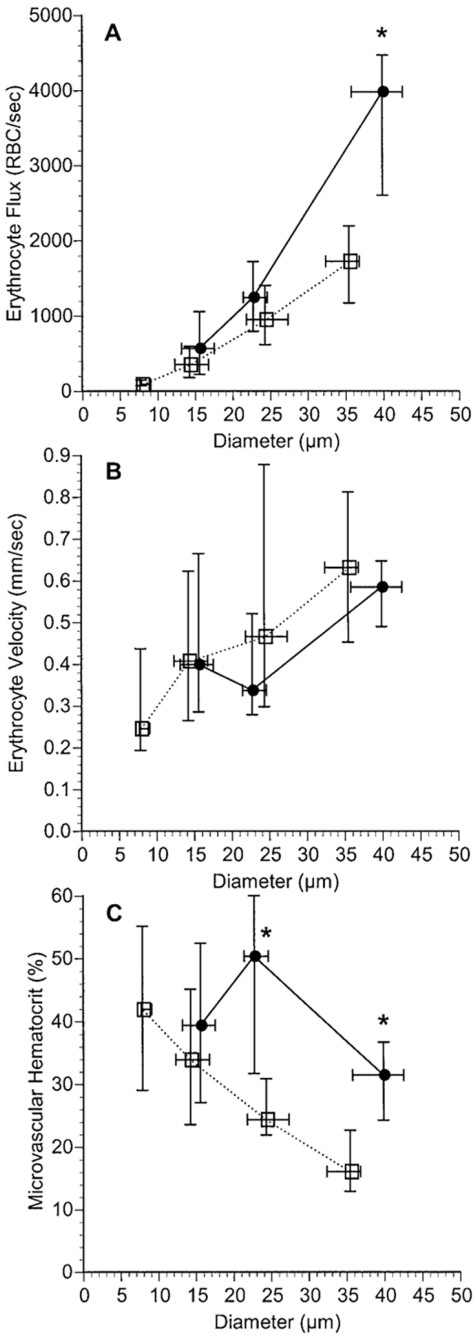

Figure 3.

Comparison of *RBC flux* (**A**), RBC velocity (**B**), and HCT_m (**C**) for a range of vessel diameters in normal choroid (□) and in choroidal melanoma (●). Data are the median ± interquartile range. The number of vessels in each diameter range (*left* to *right*) in the normal choroid was 17, 70, 41, and 24. The number of vessels in each diameter range in the choroidal melanoma was 21, 13, and 18. *Significant differences between the data from the two tissue groups ($P < 0.05$; nonparametric Mann-Whitney test).

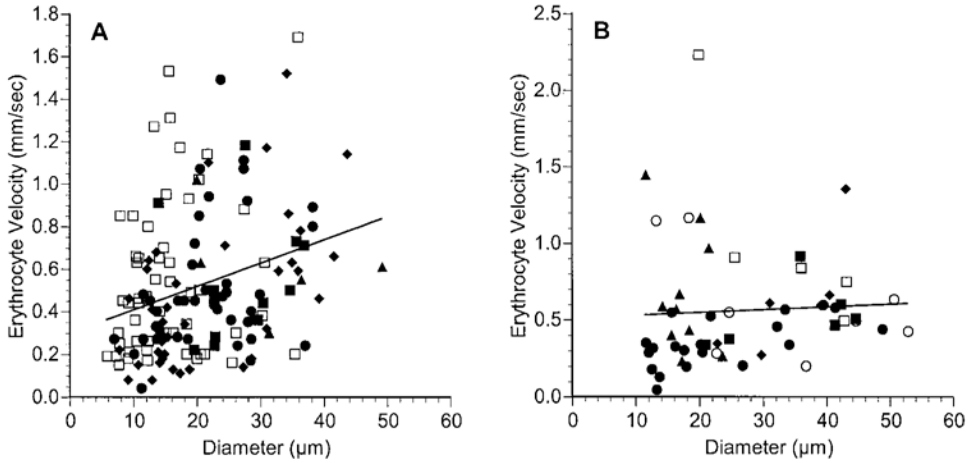

Figure 4.

RBC velocity as a function of vessel diameter in normal choroid (**A**) and in choroidal melanoma (**B**). Each rat is denoted by a different *symbol*, and each *symbol* represents a separate vessel. *Solid line*: linear regression for the data from all the rats. In normal choroid: RBC velocity = 0.011 × diameter + 0.298, n = 153 vessels in five rats, r = 0.299, P = 0.0002. In choroidal melanoma: RBC velocity = 0.0018 × diameter + 0.511, n = 55 vessels in six rats, r = 0.057, P = 0.679. Note that the scales on the ordinate axes differ.

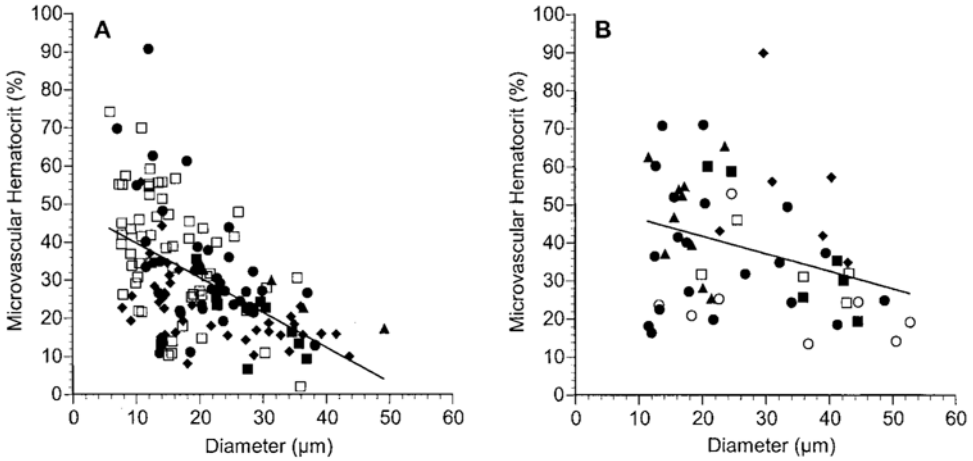

Figure 5.

Microvascular hematocrit (HCT_m) as a function of vessel diameter in normal choroid (**A**) and in choroidal melanoma (**B**). Each rat is denoted by a different *symbol*, and each *symbol* represents a separate vessel. *Solid line*: linear regression for the data from all the rats. In normal choroid: $HCT_m = -0.912 \times \text{diameter} + 48.8$, $n = 153$ vessels in five rats, $r = 0.547$, $P < 0.0001$. In choroidal melanoma: $HCT_m = -0.461$ (diameter) + 51.0, $n = 55$ vessels in six rats, $r = 0.323$, $P = 0.016$.

Table 1

Comparison of Hemodynamic Parameters in Blood Vessels of Normal Choroid and OCM-1 Choroidal Melanoma

	Diameter Range (m)			
	<10	**10–20**	**20–30**	**30–45**
RBC flux (RBC/sec)				
Normal choroid	117 ± 77 (17)	472 ± 416 (70)	1082 ± 628 (41)	1689 ± 687 (24)
OCM-1		778 ± 809 (21)	1456 ± 914 (13)	4087 ± 2484 (18)
P		0.089	0.171	**0.0002**
RBC velocity (mm/sec)				
Normal choroid	0.33 ± 0.22 (17)	0.47 ± 0.31 (70)	0.57 ± 0.35 (41)	0.70 ± 0.38 (24)
OCM-1		0.60 ± 0.54 (21)	0.43 ± 0.24 (13)	0.61 ± 0.25 (18)
P		0.610	0.215	0.596
Microvascular hematocrit (%)				
Normal choroid	42.9 ± 16.2 (17)	34.8 ± 16.1 (70)	26.2 ± 9.1 (41)	17.4 ± 7.0 (24)
OCM-1		39.8 ± 15.8 (21)	49.1 ± 20.4 (13)	32.7 ± 12.3 (18)
P		0.201	**0.0003**	**0.0001**

The values are means ± SD with the number of vessels given in parentheses. *P* reflects the significance determined by the Mann-Whitney test between the normal choroid and OCM-1 tumor results. Significant differences are in boldface.